A multiscale model of intestinal crypts dynamics

A multiscale model of intestinal crypts dynamics

Alex Graudenzi[1], Giulio Caravagna[1], Giovanni De Matteis[2], Giancarlo Mauri[1], and Marco Antoniotti[1]

[1] Dipartimento di Informatica, Sistemistica e Comunicazione, Università degli Studi di Milano Bicocca, Italy.
{alex.graudenzi, giulio.caravagna, mauri, marco.antoniotti}@disco.unimib.it

[2] Dipartimento di Matematica "F. Enriques", Università degli Studi di Milano, Italy.
giovanni.dematteis@unimi.it

Abstract. Intestinal crypts are multicellular structures the properties of which have been partially characterized, both in the "normal" and in the "transformed" development. Only in the last years there has been an increasing interest in using mathematical and computational models to achieve new insights from a "systems point-of-view". However, the overall picture lacks of a general model covering all the key distinct processes and phenomena involved in the activity of the crypt. Here we propose a new multiscale model of crypt dynamics combining Gene Regulatory Networks at the intra-cellular level with a morphological model comprising spatial patterning, cell migration and crypt homeostasis at the inter-cellular level. The intra-cellular model is a Noisy Random Boolean Network ruling cell growth, division rate and lineage commitment in terms of emergent properties. The inter-cellular spatial dynamics is an extension of the Cellular Potts Model, a statistical mechanics model in which cells are represented as lattice sites in a 2D cellular automaton successfully used to model homeostasis in the crypts.

1 Introduction

Intestinal crypts are multicellular structures are of great interest, mostly because some of their key structural and dynamical features have been quite well characterized, both in the "normal" and in the transformed development. In the latter some specific mutations or pathway alterations eventually lead to the appearance of colorectal cancer (CRC), one of the current major causes of deaths in adults [16].

In particular, the lining of the small intestine is composed by a single-layer epithelium that covers the *crypts of Lieberkhün*, i.e. invaginations in the connective tissue, which are the object of our model ([1] and references therein). 5 principal types of cells reside in the crypt: *i*) *stem cells*, *ii*) *enterocytes*, *iii*) *Goblet cells*, *iv*) *Paneth cells*, *v*) *absorptive* or *enteroendocrine*. Cell populations are segregated and sorted in well-defined compartments and the (fast) turnover process is accomplished through a very complex coordinate migration process. In particular,

stem cells are positioned in the lower part of the crypt, within a specific niche, intermingled with Paneth cells, and the other types of cells reside in the upper portion of the crypt. The overall dynamics is a coordinate upward migration of cells dividing in transit amplifying stage, moving from the stem and Paneth cell niche toward the top of the crypt. A deeply schematized representation of the lineage commitment tree is shown in Figure 1, while a representation of the crypt morphology and of the main pathways involved in its dynamics is shown in Figure 2. For a more detailed description of the intestine biology the reader is referred to [7] and to the further references therein.

Only in the last years there has been an increasing number of attempts to use mathematical and computational models to achieve new insights on this system from a "systems point-of-view" and, in this regard, in [7] we reviewed the existing models designed for the description of the morphology and the morphogenesis of the intestinal crypts. The review highlighted the lack of a general model covering all the distinct processes and phenomena involved in the activity of the crypt and, so, a holistic system-based picture of the overall dynamics is still missing.

To try to fill this gap, we adopted a *multiscale modeling* methodology to describe the crypts. Multiscale modeling is intended to deal with the separation of the spatial and temporal scales entailed in the distinct cellular and intercellular processes, at different abstraction levels. Thus, the notion of *hierarchy* becomes fundamental to describe all the levels of the crypt organization, from the intracellular (e.g. gene regulation, intra-cellular communication), to the inter-cellular (e.g. signaling pathways, inter-cellular communication, cell-environment communication) and the tissue level (e.g. spatial patterning, crypt homeostasis).

Setting on these premises, the aim of this paper is to propose a new multiscale computational model integrating a general model of gene regulatory network (GRN) with a spatial/morphological model of crypt dynamics. The model should be capable of covering a broad range of experimentally observed phenomena, both from the *qualitative* and the *quantitative* point of view. Up to now our contribution, which is developed within the RetroNet project (see Acknowledgments), is the model construction. Its implementation and the subsequent analyses are the next expected steps for the same project. By combining low and high-level dynamics we expect that our model permits a better understanding of key dynamical phenomena such as cell sorting, migration, niche maintenance and general homeostasis. Furthermore, we think that the model should permit to investigate the repercussion of different kinds of gene-level perturbations on the overall dynamical behaviour, with reference to the emergence of cancer.

2 Modeling the internal dynamics as NRBNs

The internal dynamics of each cell is modeled with a *Noisy Random Boolean Network* (NRBN) [24,26], a generalization of classical RBNs [18,17,19], a highly abstract and general model of gene regulatory network, which was proven to reproduce several biological properties of real networks [28,29,27]. As proposed by Villani et al. [30], NRBNs are particularly effective in describing some of the

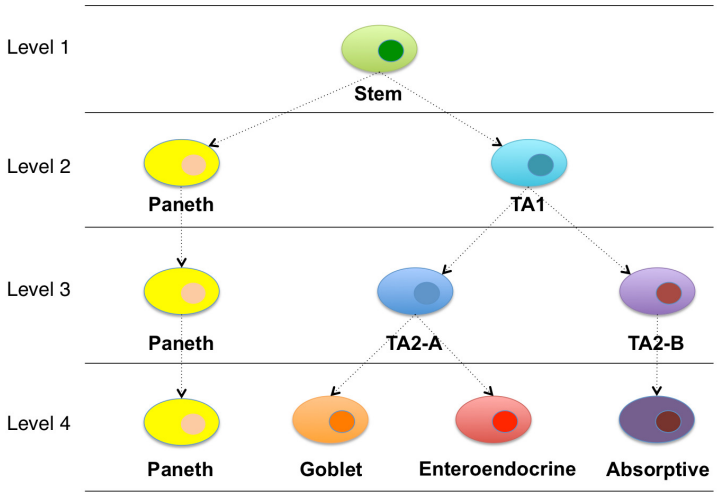

Fig. 1. Schematic representation of the crypt differentiation tree. Stem cells (St) are the root of the tree, while the 4 differentiated cell types (i.e. Paneth (Pa), Goblet (Go), enteroendocrine (Ee), absorptive or enterocyte (Ec)) are the leaves. TA stands for transit amplifying stage, which is known to be the intermediate state between stem and fully differentiated stages.

most relevant features of the differentiation process, in detail: *i*) the definition of a specific stem cell type which can generate any other type of cell (*totipotent*) or a subset of them (*pluripotent*) [1], usually through transit amplifying stages; *ii*) the presence of a (recursive) *stochastic differentiation* process [15,6,13] according to which a population of identical stem cells generate different cell types, which in turn generate more differentiated cell types and the process repeats; *iii*) the *deterministic differentiation* [31], according to which there exist specific signals triggering, through the mutation of specific genes, the development of a stem cell along a specific differentiation pathway.

Background: Classical and Noisy RBNs. For an exhaustive description of the classical RBN model please refer to [2]. Here we will outline the key features of the Noisy Random Boolean Network model.
Classical RBNs are directed graphs in which nodes represent genes and their Boolean value stands for the corresponding activation or inactivation, while the edges symbolize the paths of regulation. A Boolean updating function is associated to each node and the update occurs synchronously at discrete time step for each node of the network, according to the value of the inputs nodes at the previous time step. Since the network dynamics is discrete, synchronous and deterministic the only asymptotic states (i.e. the *attractors*) of the system are cycles (and fixed points).
The rationale at the base of the development of the Noisy Random Boolean Networks model (NRBN) is that noise plays a major role in numerous cellular

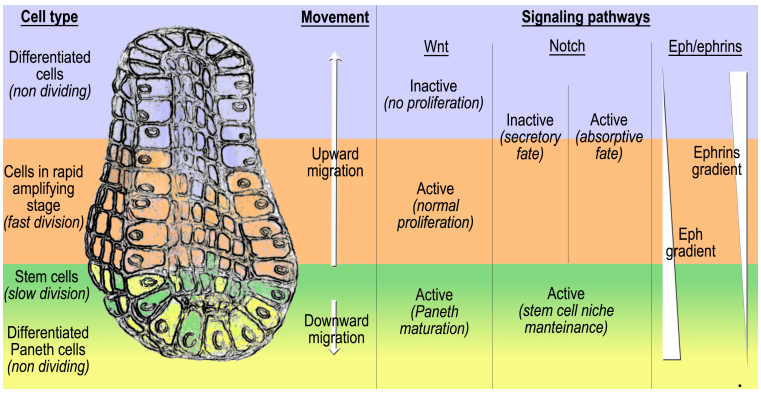

Fig. 2. Representation of the crypt morphology, with specific regard to the migration directions and the signaling pathways involved in its dynamics. Four types of cells are represented: Paneth cells (yellow), stem cells (green), cells in transit amplifying stage (orange) and differentiated (i.e. Goblet, enteroendorcrine and enterocyte) cells (light blue). All cells but stem and Paneth migrate upward. The three major signaling pathways involved in the crypt activity are the Wnt, the Notch and the Eph/ephrins pathways. The complex interplay among them, with reference to the repercussions on the various phenomena in the crypt, is schematized in this figure, taken from [7].

phenomena [23,5,22,8] and, above all, it is supposed to drive the differentiation process [21,14,12]. Classical RBNs are fully deterministic and, hence, they do not properly take this aspect into account.

In the classical version of the RBN model cell types are associated to attractors, given that all the different cells of an organism share the same gene network and the differences in the cell types can be interpreted as different gene activation patterns. Nevertheless, attractors in RBNs are, in general, deeply sensitive to the introduction of noise, intended as perturbations of the value of one or more nodes. To this end, Ribeiro and Kauffman proposed a more sound approach to connect attractors and cell types [25] and, successively, Villani *et al.* developed a further refinement of the idea [30], which is described in the following.

Given a specific RBN, a temporary flip[3] is performed for each node in each state of each attractors, detecting all the possible transitions from one attractor to another one and, consequently, drawing the so-called *attractor transition network* (ATN). NRBNs rely on the assumption that the level of noise is sufficiently low to allow the system to reach its (new or old) attractor before another flip occurs. This assumption is endorsed by simulations showing that the number of steps to skip from one attractor to another one is usually small [30].

A *threshold* is then introduced to remove from the ATN those transitions that are considered too rare to occur, i.e. it is reasonable to think that some "jumps"

[3] When a flip in the $i-$th gene is performed the value σ_i is complemented, the flip lasts 1 time step in the time-evolution of the network. This is indeed the smallest perturbation which can affect a Boolean network.

are too rare to happen with a significant probability within the lifetime of the cell and, therefore, we consider *threshold-dependent ATNs*. Accordingly, a *Threshold Ergodic Set* (TES in brief or TES_δ when $\delta \in [0,1]$ is the threshold) is a set of attractors in which the dynamics of the system continue to transit, in the long run, due to random flips (i.e. noise) or, using the graph theory terminology, a *strongly connected component* (SCC) in the threshold-dependent ATN.
Formally, let $\mathcal{A} = \{\alpha_1, \alpha_2, \ldots\}$ be the finite set of attractors of a NRBN. By performing for each attractor and gene a single flip , and by observing which potentially attractor is reached, it is possible to define a weighed transition graph among attractors. By using the normalized frequency of such switches it is possible to determine a stochastic matrix $P_\mathcal{A} \subseteq [0,1]^{|\mathcal{A}|\times|\mathcal{A}|}$ where $p_{i,j}$ determines the probability of switching from attractor α_i to attractor α_j, and $\sum_{j=1}^{|\mathcal{A}|} p_{i,j} = 1$ for $i = 1, \ldots, |\mathcal{A}|$. Given a threshold δ an attractor α_j is δ-reachable from another attractor α_j if $p_{i,j} \leq \delta$. Besides, α_j is δ-reachable from α_i if there exist a path connecting α_i to α_j through transitions between pairs of δ-reachable attractors. A set $\theta \subseteq \mathcal{A}$ is a TES_δ if (i) any $\alpha_i \in \theta$ is δ-reachable from any other member of the TES. When the threshold is 0 a unique TES, which is indeed an Ergodic Sets in the sense of [25], is usually found. When the threshold is smoothly increased the TESs divide into smaller TESs, i.e. composed by less attractors, up to the point in which the TESs are indeed the attractors.

The model. Here we assume that each TES of a NRBN represents a specific cell type characterized by a peculiar noise resistance, as indicated by the relative threshold. The degree of differentiation (i.e. highly differentiated against less differentiated) relates to the possibility for the cell in its attractor to roam in a wider or smaller portion of the phase space (i.e. the size of the TESs which decreases as the threshold increases).
At the best of our knowledge, in fact, less differentiated cells (e.g. stem cells) show fewer control mechanisms against noise (e.g. copy errors) and, thus, we characterize them by a smaller threshold allowing them for roaming in a wider portion of the phase space [30]. On the opposite, cells in a more differentiated state present more refined control mechanisms and, consequently, are associated to higher thresholds which actually prevent random fluctuations [22].
In the construction of a suitable NRBNs to be used in the model, we impose some constraints based on the current biological knowledge of real gene networks.
The main constraints concern the topology and the choice of the updating boolean functions. In regard to the former, we design NRBNs with n genes and *scale-free* topology [3]. More precisely, the fraction of nodes in the network having k connections to other nodes follows $ck^{-\gamma}$, for large values of k, where c is a normalization constant and $\gamma \approx 2.3 \div 2.5$ is a parameter whose value relates to the structure of many biological networks, including GRNs [4]. On the other hand, we impose a constraint on the choice of the boolean functions, based on the biological plausibility of updating functions in GRN models [11]. In particular we impose that all the functions must be canalyzing [20].

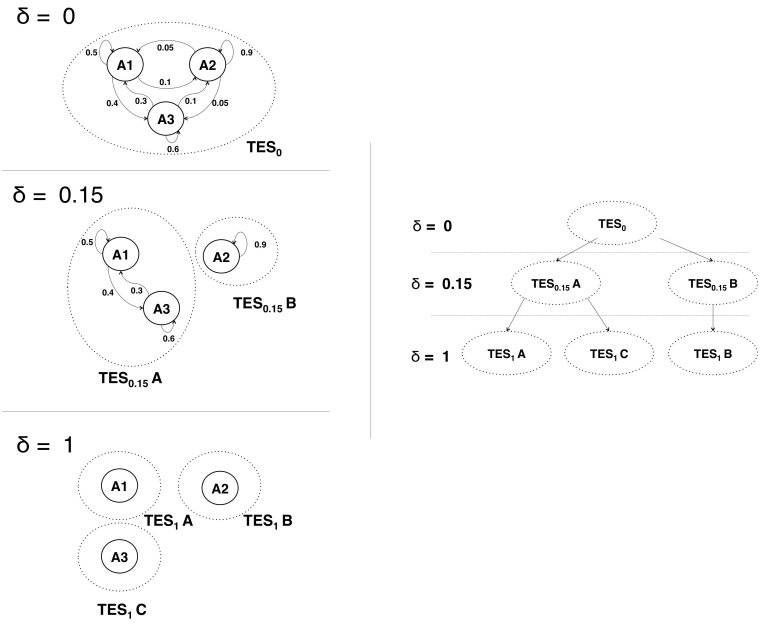

Fig. 3. An example of the threshold-dependent ATN and the corresponding tree-like TES landscape. The circle nodes are attractors of an example NRBN, the edges represent the relative frequency of transitions from one attractor to another one, after a 1 time step-flip of a random node in a random state of the attractor (performed an elevated number of times). In this case we show three different values of threshold, i.e.: $\delta = 0$, $\delta = 0.15$ and $\delta = 1$. TESs, i.e. strongly connected components in the threshold-dependent ATN are represented through dotted lines and the relative threshold is indicated in the subscripted index. In the right diagram it is shown the tree-like representation of the TES landscape.

Search of the suitable NRBNs. In our model we associate totipotent stem cells with TESs at threshold 0, cells in a pluripotent or multipotent state (i.e. transit amplyfing stage or intermediate state) with TESs with a larger threshold composed by one or more attractors, while completely differentiate cells (i.e Paneth, Goblet, enteroendocrine and enterocyte) correspond to TESs with the highest threshold, usually composed by single attractors.
It should be clear at this point that an *a priori* choice of a specific NRBN does not guarantee the existence of the TES and thresholds corresponding to the desired differentiation tree (e.g. Figure 1). In addition, this would contradict our choice of not imposing specific detailed assumptions concerning the interaction which drive the modeled phenomena. As a consequence, we must perform a search among plausible NRBNs to match the outlined acceptability criteria. Once the suitable NRBNs are collected, they can be used to complete and analyze the whole model, as we shall see in the next sections.
Summarizing, we (a) generate a scale-free NRBN with canalizing boolean func-

tions, which also are generated at random. Then, we (b) sample a possibly exhaustive number of initial conditions for the network. We (c) find a subset of its attractors by flipping the genes[4], i.e. a subset of $\mathcal{A}$ which is dependent on the number of different sampled initial configurations, and we define the matrix $P_{\mathcal{A}}$ describing the stability of all the attractors. For a $\delta \in [0,1]$ we define the prune of $P_{\mathcal{A}}$ to be the matrix $P_{\geq\delta}$ whose elements $p'_{i,j}$ are equal to the corresponding $p_{i,j}$, the elements of $P_{\mathcal{A}}$, if $p_{i,j} > \delta$, and $p'_{i,j} = 0$ otherwise. The prune completes once we re-normalize the matrix, since otherwise it does not represent a correct stochastic matrix, which is actually required in the next part of the model, as we shall see later. As expected, different TESs are determined by different values of δ and $P_{\geq 0} = P_{\mathcal{A}}$ and $P_{\geq 1}$ is the zero matrix. We denote with $\Theta_{\geq\delta}$ the set of TESs for matrix $P_{\geq\delta}$. Last step (d) requires to find a set of suitable thresholds (i.e. $\delta_0 < \delta_1 < \delta_2 < \delta_3$ with $\delta_0 = 0$) that implicates the perfect match between the graph structure of the differentiation tree in Fig. 1 and that of the tree-like representation of the TES landscape (e.g. Fig. 3). This is done by means of a rather complicated procedure (not presented here) at the end of which all the distinct threshold-dependent ATNs are defined. Once an NRBN with these peculiar features has been determined, this internal model can be used to rule several key cellular processes involved in cell division and differentiation.

The NRBN dynamics. As far as the NRBN dynamics is concerned, when the simulation starts a random attractor of the specific TES is assigned to every cell, according to its type. We remark that all the cells are characterized by a structurally identical NRBN (i.e. same genome), even if their state can belong to different portions of the state space. While time advances, if no NRBN-level perturbations are performed the cell potentially resides in the same attractor, unless higher-level events which shall be discussed in the next sections happen. At this level noise is accounted as the probability p that each node has to perform a transient flip at any time step of the dynamics. Instead of running the step-by-step NRBN dynamics we make use of the already mapped TES landscape and of the relative frequency of transition among the attractors. In this way NRBNs can jump from one attractor to another one within their own TES, according to the peculiar level of noise, in the course of the simulation time.

3 Modeling the spatial/morphological dynamics

We decided to adopt an evolution of the original *Cellular Potts Model* (CPM) [9,10] on the basis of the work by Wong et al [32], who extended the original model to a 2-D lattice with periodic boundary conditions, representing the (unrolled) surface of the crypt with a certain degree of approximation, accounting for cell types and sizes.

[4] To draw the *exact* ATN all the possible flips of all the nodes in all the states of all the attractors should be performed [30]. Since even relatively small networks have huge state spaces, an exact sampling is practically unfeasible. Nonetheless, it is possible to draw the ATN up to a desired precision.

The model considers a population of k *cells* disposed over a 2-D *lattice of positions* $L \in \{1, \ldots, k\}^{n \times m}$, i.e. a cellular automaton, where $l_{i,j} = w$ if the lattice position (i, j) is occupied by cell w. Cells are delimited by connected *domains*, namely cell w is determined by the positions $\mathcal{C}(w) \stackrel{\text{def}}{\equiv} \{l_{i,j} = w \mid (i, j) \in L\}$. If a set of cell types T is considered, a lattice site is naturally extended to $l_{i,j} = (w, \tau)$ if the position is occupied by cell w, and cell w has type $\tau \in T$.
In CPM cells are expected to rearrange (i.e. via *cell sorting*) and change shape according to an energy gradient. Potts assigned to each lattice configuration L a *hamiltonian energy* $\mathcal{H} : \mathbb{I}^{n \times m} \to \mathbb{R}$ denoted $\mathcal{H}(L)$. In practice, we arbitrarily define $\mathcal{H}$ as far as we can describe a process in terms of a real or effective potential energy. In the subsequent section we will describe the hamiltonian used in our model (Eq. 7).
The time-evolution of a lattice occurs through a series of *flips*. Given a lattice L, we define the flip of a position (x, y) to a cell w to be the new lattice L', that is

$$L' \stackrel{\text{def}}{\equiv} L[w \leftarrow (x, y)] \quad \text{where} \quad l'_{i,j} = \begin{cases} w & \text{if } (i, j) = (x, y) \\ l_{i,j} & \text{otherwise} \end{cases}$$

where $l'_{i,j}$ and $l_{i,j}$ are the same position in L' and L, respectively.
The simulation of the CPM works according to a Metropolis-like algorithm. In the following, we denote with $L(t)$ the lattice at time t. Given the $n \times m$ lattice $L(t)$, at each step a position (i, j) is chosen with uniform probability, i.e. $i \sim U[1, n]$ and $j \sim U[1, m]$. Moreover, a neighbour $w \in \mathcal{N}(i, j)$, uniformly distributed on the set $\mathcal{N}(i, j)$ is chosen and is used as a candidate flip. The algorithm probabilistically accepts or rejects the flip, i.e. $L'(t) \stackrel{\text{def}}{\equiv} L[w \leftarrow (i, j)]$, according to the hamiltonian energy evaluated in both lattices. Formally, $L'(t)$ is accepted or rejected according to the probability distribution $\mathcal{P}(L'(t))$ where

$$P(L'(t)) \stackrel{\text{def}}{\equiv} \min \left\{ 1, \exp\left(-\frac{\Delta\mathcal{H}}{k_B T} \right) \right\} \tag{1}$$

for $k_B T > 0$, and

$$P(L'(t)) \stackrel{\text{def}}{\equiv} \begin{cases} 0 & \text{if} \quad \Delta\mathcal{H} > 0 \\ \frac{1}{2} & \text{if} \quad \Delta\mathcal{H} = 0 \\ 1 & \text{if} \quad \Delta\mathcal{H} < 0 \end{cases}. \tag{2}$$

for $k_B T = 0$. These equations account for the change of energy induced by the flip, the temperature T and the Boltzmann constant k_B.
Intuitively, the goal is to minimize the energy of the lattice by re-ordering the cells. A computation starting at time t_s and ending at time t_e performs $t_e - t_s$ MonteCarlo steps (MCSs) each one attempting nmk random flips, where $k \in \mathbb{I}$ is an arbitrary constant. Once all the attempts of flips are finished, the new lattice $L(t+1)$ is determined as a result of all the accepted flips. Formally, such process is a Discrete Time Markov Chain.
We remark that we introduced some modifications to Wong's model. In detail, we use a distinct set of cell types $T = \{\text{St}, \text{TA1}, \text{TA2-A}, \text{TA2-B}, \text{Pa}, \text{Go}, \text{Ec}, \text{Ee}\}$

which indeed corresponds to the differentiation tree that describes the crypt lineage commitment presented in Figure 1. Besides, while in the original model the growth and division dynamics are prefixed and occur as described above, in the multi-scale model they are be strictly interconnected with the low-level dynamics, i.e. thus driven by the NRBN, as it will be explained in the next section.

4 Linking NRBNs and CPM: the multi-scale model

Three major processes of the cellular activity are ruled by the internal dynamics of the NRBNs, hence influencing the CPM spatial dynamics: (*i*) *the length of the cell cycle*, which is tied to the weighted length of the attractors belonging to the corresponding TES, thus being an emergent property; (*ii*) *the growth rate of the size of the cell*, which is assumed to linearly increase up to the doubling of the original size, so that when the size is doubled (at the end of the cycle) the cell divides and differentiates; (*iii*) *the lineage commitment tree*, which depends on the structure of the landscape of the attractors and, consequently, of the TESs so that the differentiation bifurcations consequently depend on the position in which the dynamical trajectory of the system is when the cell divides.

Cell cycle length. In regard to the length of the cell cycle, for a cell of type τ_i, whose NRBN threshold is δ_i, we consider its biggest TES in $\Theta_{\geq\delta_i}$ and the stochastic matrix $P_{\geq\delta_i}$ restricted to the states and the transitions regarding only the attractors in the TES and, with abuse of notation, we still denote it as $P_{\geq\delta_i}$. As we said, $P_{\geq\delta_i}$ is a Discrete-Time Markov Chain (DTMC). By standard DTMC theory if it is possible to go from each state, in any number of steps, to every other state, then the chain is *ergodic* and, obviously, this is the case by the definition of TESs. This implies also the *irreducibility* of $P_{\geq\delta_i}$. It holds that the *stationary probability distribution* π_i of an irreducible DTMC in an ergodic set of states is unique and is the fixed point of: $\pi_i P_{\geq\delta_i} = \pi_i$, where $P_{\geq\delta_i}$ is the stochastic matrix for the considered TES. For the cell of type τ_w we determine the length ℓ_w of its cell cycle as

$$\ell_w \stackrel{\text{def}}{\equiv} \sum_{\alpha_j \in \theta} \eta_j \pi_i(\alpha_j) \tag{3}$$

where η_j is the length of attractor α_j. The length of the cell cycle in CPM is then an emergent property of the NRBN dynamics. This requires the conversion between the time-scales of the internal and external models which, at the best of our knowledge, is a new result.

Time-scales conversion. We highlight that the difference between the time-scales of the NRBN steps with respect to the CPM steps is the key property of the multiscale model. Therefore, we link the time scale of the internal dynamics (i.e. the NRBN steps) with the time scale of the MonteCarlo simulation (i.e. the

CPM steps). Along the line of Wong's simulation experiments [32] we consider that: (*i*) 10 MonteCarlo steps (MCSs) correspond to 1 hour of biological time; (*ii*) the length of a cell cycle Δt_{cycle} is in the range $12 \div 17$ hours, according to the different cell types, that is it takes in between 120 and 170 MCSs; (*iii*) the natural unit for l_w is one NRBN step of the internal dynamics. So, we end up with the following conversion

$$1 \text{ RBN step} = \frac{\Delta t_{cycle}}{\ell_w} \text{MCSs} = \frac{120 \div 170}{\ell_w} \text{MCSs}\,. \tag{4}$$

Cell size dynamics. The *current area* of a cell w in a lattice is defined as

$$a(w) \stackrel{\text{def}}{\equiv} \sum_{\mathcal{C}(w)} a = |\mathcal{C}(w)|a$$

where a is a basic quantity of area assigned to a single lattice position. This quantity dynamically evolves in the lattice according to the performed flips.
To each cell w of type τ a standard area $A(\tau, w)$ is associated, representing the area of any newborn cell of that kind. In addition, we introduce a time-dependent *target area* $A(\tau, w, t)$ which is evolving according to the dynamics of the underlying NRBN. The target area represents the growing cell size during its cycle and as if it was *mechanically isolated*, that is with no contact interaction with neighbor cells.
We now link the dynamical evolution of the target area $A(\tau, w, t)$ to the length of the cell cycle ℓ_w as defined in equation (3). We assume the doubling of the volume of a cell to happen after a complete cell cycle and we consider a *linear* growth for all the cycle. We have that, if t_0 is the time at which a cell starts its cycle, then

$$A(\tau, w, t) = \begin{cases} A(\tau, w), & \text{if } t = t_0 \\ A(\tau, w, t-1) + \mu \left[\frac{A(\tau,w)}{\ell_w}\right]_{int} & \text{otherwise} \end{cases} \tag{5}$$

or, alternatively

$$A(\tau, w, t) = \begin{cases} A(\tau, w), & \text{if } t = t_0 \\ A(\tau, w) + \mu \left[(t - t_0)\frac{A(\tau,w)}{\ell_w}\right]_{int} & \text{otherwise} \end{cases} \tag{6}$$

where $\mu = 0$ for non-dividing cells and $\mu = 1$ for proliferative cells. Notice that in (5) and (6) $[\_]_{int}$ denotes the nearest-integer function. This latter function comes from considering an integer number of incremental pixels in the cell area as a consequence of our lattice discretization. The hamiltonian of the system is then defined by

$$\begin{aligned} \mathcal{H}(L) \stackrel{\text{def}}{\equiv} & \sum_{(i,j)\in L} \left(\sum_{(i',j')\in\mathcal{N}(i,j)} J(\tau, \tau')\,(1 - \delta(w, w')) \right) \\ & + \lambda \sum_{\tau \in T} [a(w) - A(\tau, w, t)]^2 \,\text{Heav}(A(\tau, w, t)) \end{aligned} \tag{7}$$

if $l_{i,j} = (w, \tau)$ and $l_{i',j'} = (w', \tau')$, where $\mathcal{N}(i, j)$ denotes the neighborhood of position (i, j) according to some distance metrics (e.g. Von Neumann neighborhood); λ is the strength of size constraint which is proportional to the capacity to deform the cells membrane; $J(\tau, \tau')$ is the surface energy between cells of type τ and τ', as derived from the symmetric matrix $J : T \times T \to \mathbb{R}$, which denotes the energy required by cell of type τ to adhere to one of type τ' (an adhesion constant matrix is given, for instance, in [32])[5]. Biological aggregates are also surrounded by a hosting fluid (ECM) which is usually marked with a special cell type which has unconstrained area. Therefore, the medium target area is set to be negative and the corresponding area constraint is suppressed by including the Heaviside function, i.e. Heav$(A(\tau, w, t))$.

Cell division and differentiation dynamics. Finally, when one cell cycle is concluded (i.e. after ℓ_w RBN time steps) and the size of the cell has doubled its target size (i.e. $2A(\tau, w)$) we assume that the cell instantaneously divides in two on the lattice and differentiates.
For the two daughter cells the TES threshold is automatically increased to the subsequent level, which is chosen as indicated in Section 2, implying the hypothesized variation in the level of noise resistance and control [22]. The differentiation direction and the new TES to which the daughters will belong is chosen looking at the attractor in which the progenitor cell is found at the moment of division. Notice that NRBNs wander in the TES space according to the particular level of noise p introduced in Section 2. In this regard, the process of stochastic differentiation is effectively depicted by the model.

5 Conclusions

The objective of this work was to present a novel multi-scale model describing the dynamics of intestinal crypts. The main novelties of the model can be summarized as follows:

- First, the model describes in a original way phenomena and processes occurring at different spatial/temporal scales, i.e. the low-level mechanisms of gene regulation on the on the one hand, and the high-level phenomena regarding the crypt homeostasis and the spatial patterning of cells, on the other hand. Key cellular processes, e.g. cell growth and differentiation, are at the center of a continuos exchange of information among the levels, on the basis of the conversion of the different time scales shown in Section 4.
- Another important novelty resides on the attention casted on the concept of emerging dynamical behaviour. The dynamics of both the low- and the high-level models are strictly related to the emergence of particular gene activation patterns (i.e. attractors), which eventually determines the general

[5] Notice that the use of the delta function (i.e. Kronecker symbol) ensures that only the surface sites between different cells contribute to the adhesion energy.

activity and fate of the system. In analogous models, processes such as cell cycle or cell division are usually prefixed, depending on external parameters, and do not emerge from the dynamics.
- The comparison of statistical analyses of ensembles of NRBNs designed with biologically plausible structural parameters with experimental data concerning the overall activity of the crypt will allow to achieve new insights on the generic properties of such a system and on other possibly not expected biological constraints and mechanisms.
- The possibility of simulating various perturbations at the gene level allows innovative possibilities in investigating how biological noise and mutations can spread through complex biological system, eventually leading to functional disorders and to the emergence of tumors and cancers.

Several simulations on the model are underway, with the goal of providing a more exhaustive picture of the complex interplay that regulates the crypt activity and homeostasis.

6 Acknowledgments

We wish to thank the Regione Lombardia for its support of this research and the RetroNet project through the grant 12-4-5148000-40; U.A 053.

References

1. Alberts, B., Johnson, A., Lewis, J., Raff, M., Roberts, K., Walter, P.: Molecular Biology of the Cell, fifth edition edn. Garland Science (2007)
2. Aldana, M., Coppersmith, S., Kadanoff, L.: Boolean dynamics with random couplings. In: E. Kaplan, J. Marsden, K. Sreenivasan (eds.) Perspectives and Problems in Nonlinear Science, Springer Applied Mathematical Sciences Series. Springer, New York (2003)
3. Barabasi, A.L.: Linked: The New Science of Networks. Perseus Publishing (2002)
4. Barabasi, A.L., Oltvai, Z.: Network biology: understanding the cell's functional organization. Nature Reviews Genetics **5**, 101–113 (2004)
5. Blake, W., et al.: Noise in eukaryotic gene expression. Nature **422**, 633–637 (2003)
6. Chang, H., et al.: Transcriptome-wide noise controls lineage choice in mammalian protenitor cells. Nature **453**, 544–548 (2008)
7. De Matteis, G., Graudenzi, A., Antoniotti, M.: A review of spatial computational models for multi-cellular systems, with regard to intestinal crypts and colorectal cancer development. Journal of Mathematical Biology **Submitted**, – (2012)
8. Eldar, A., Elowitz, M.: Functional roles for noise in genetic circuits. Nature **467**, 167–173 (2010)
9. Graner, F., Glazier, J.: Simulation of biological cell sorting using a two-dimensional extended potts model. Physical Review Letters **69**, 2013–2017 (1992)
10. Graner, F., Glazier, J.: Simulation of the differential adhesion driven rearrangement of biological cells. Physical Review E **47**, 2128–2154 (1993). URL http://graner.net/francois/publis/glazier_rearrangement.pdf

11. Grefenstette, J., Kim, S., Kauffman, S.: An analysis of the class of gene regulatory functions implied by a biochemical model. Biosystems **84**, 81–90 (2006)
12. Hoffman, M., et al.: Noise driven stem cell and progenitor population dynamics. PLoS ONE **3**, e2922 (2008)
13. Huang, S.: Reprogramming cell fates: reconciling rarity with robustness. Bioessays **31**, 546–560 (2009)
14. Huang, S., et al.: Bifurcation dynamics in lineage-commitment in bipotent progenitor cells. Dev. Biol. **305**, 695–713 (2007)
15. Hume, D.: Probability in transcriptional regulation and its implications for leukocyte differentiation and inducible gene expression. Blood **96**, 2323–2328 (2000)
16. Jemal, A., Siegel, R., Xu, J., Ward, E.: Cancer statistics 2010. CA Cancer J. Clin. **60**, 277–300 (2010)
17. Kauffman, S.: Homeostasis and differentiation in random genetic control networks. Nature **224**, 177 (1969)
18. Kauffman, S.: Metabolic stability and epigenesis in randomly constructed genetic nets. J. Theor. Biol. **22**, 437–467 (1969)
19. Kauffman, S.: At home in the universe. Oxford University Press (1995)
20. Kauffman, S., Peterson, C., Samuelsson, B., Troein, C.: Genetic networks with canalyzing boolean rules are always stable. Proc. Natl Acad. Sci. USA **101**, 17,102–7 (2004)
21. Kupiec, J.: A probabilist theory for cell differentiation, embryonic mortality and dna c-value paradox. Speculations Sci.Technol. **6**, 471–478 (1983)
22. Lestas, I., et al.: Noise in gene regulatory networks. IEEE Trans. Automat. Contro. **53**, 189–200 (2008)
23. Mc Adams, H., Arkin, A.: Stochastic mechanisms in gene expression. Proc. Natl Acad. Sci. USA **94**, 814–819 (1997)
24. Peixoto, T., Drossel, B.: Noise in random boolean networks. Phys. Rev. E **79**, 036,108–17 (2009)
25. Ribeiro, A., Kauffman, S.: Noisy attractors and ergodic sets in models of gene regulatory networks. J. Theor. Biol. **247**, 743–755 (2007)
26. Serra, R., Villani, M., Barbieri, A., Kauffman, S., Colacci, A.: On the dynamics of random boolean networks subject to noise: attractors, ergodic sets and cell types. J. Theor. Biol. **265**, 185–193 (2010)
27. Serra, R., Villani, M., Graudenzi, A., Kauffman, S.: Why a simple model of genetic regulatory networks describes the distribution of avalanches in gene expression data. J. Theor. Biol. **249**, 449–460 (2007)
28. Serra, R., Villani, M., Semeria, A.: Genetic network models and statistical properties of gene expression data in knock-out experiments. J. Theor. Biol. **227**, 149–157 (2004)
29. Shmulevich, I., Kauffman, S., Aldana, M.: Eukaryotic cells are dynamically ordered or critical but not chaotic. Proc. Natl Acad. Sci. USA **102**, 13,439–44 (2005)
30. Villani, M., Barbieri, A., Serra, R.: A dynamical model of genetic networks for cell differentiation. PLoS ONE **6**(3), e17,703. doi:10.1371/journal.pone.0017,703 (2011)
31. Wolpert, L.: Do we understand development? Science **266**, 571–572 (1994)
32. Wong, S.Y., Chiam, K.H., Lim, C.T., Matsudaira, P.: Computational model of cell positioning: directed and collective migration in the intestinal crypt epithelium. Journal of The Royal Society Interface **7**(Suppl 3), S351–S363 (2010). DOI 10.1098/rsif.2010.0018.focus